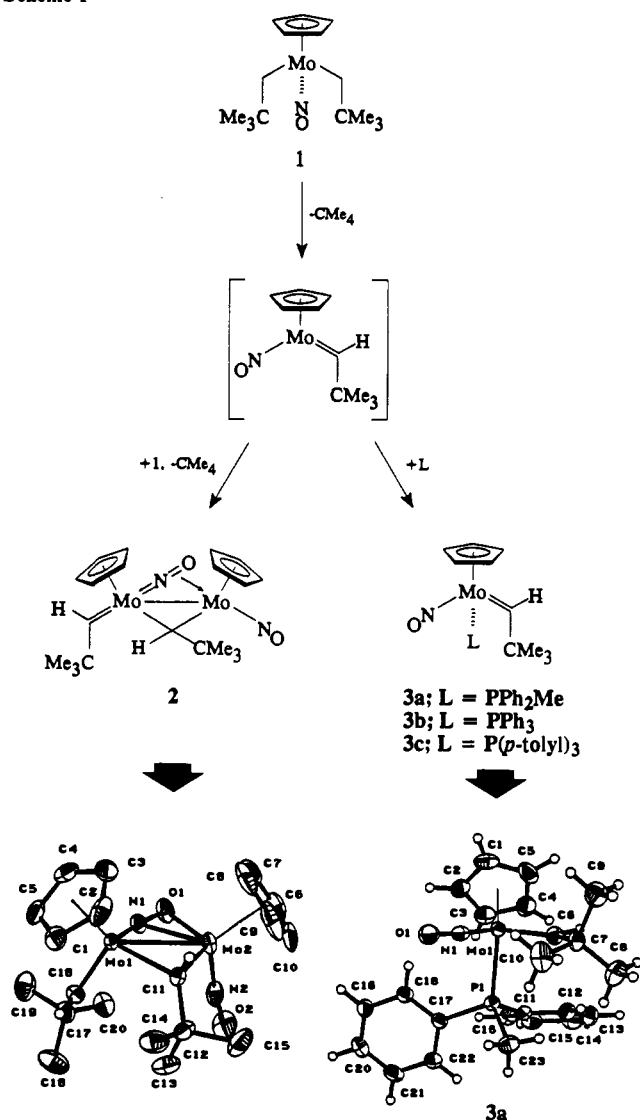


Scheme 1



essentially linear [Mo(1)–N(1)–O(1) = 165.5 (2)°] and is symmetrically disposed with respect to Mo(2) [Mo(2)–N(1) = 2.187 (3) Å and Mo(2)–O(1) = 2.149 (2) Å]. The spectroscopic properties of **2** confirm that the solid-state molecular structure persists in solution. Thus, its IR spectrum in CH<sub>2</sub>Cl<sub>2</sub> exhibits terminal (1594 cm<sup>-1</sup>) and bridging (1328 cm<sup>-1</sup>) nitrosyl bands, and its <sup>1</sup>H and <sup>13</sup>C NMR spectra exhibit two sets of equal intensity Cp, CH, and CMe<sub>3</sub> resonances.<sup>4</sup>

The transformation of **1** into **2** is remarkable, but it also appears to be quite complex. Consistent with the transient formation of CpMo(NO)(=CHCMe<sub>3</sub>) from **1**, thermolysis of **1** in the presence of phosphines, L, produces the adducts CpMo(NO)(=CHCMe<sub>3</sub>)(L) [**3a**, L = PPh<sub>2</sub>Me; **3b**, L = PPh<sub>3</sub>; **3c**, L = P(*p*-tolyl)<sub>3</sub>].<sup>4,10</sup> The intramolecular dimensions of **3a**,<sup>5</sup> as established by X-ray diffraction, resemble those exhibited by the related [CpRe(NO)(=CHPh)(PPh<sub>3</sub>)]<sup>+</sup> cation.<sup>11</sup>

(9) For comparison, other long N–O bonds are as follows: (a) 1.247 (5) Å for the μ<sub>3</sub>-NO of Cp<sub>3</sub>Mn<sub>3</sub>(NO)<sub>4</sub> (Elder, R. C. *Inorg. Chem.* 1974, 13, 1037); (b) 1.271 (7) Å for the μ<sub>4</sub>-η<sup>2</sup>-NO of a mixed Co/Mo cluster (Kyba, E. P.; Kerby, M. C.; Kashyap, R. P.; Mountzouris, J. A.; Davis, R. E. *J. Am. Chem. Soc.* 1990, 112, 905); and (c) 1.47 (1) Å for CpRe(PPh<sub>3</sub>)(SiMe<sub>2</sub>Cl)(NO–BCl<sub>3</sub>) (Lee, K. E.; Arif, A. M.; Gladysz, J. A. *Inorg. Chem.* 1990, 29, 2885).

(10) To the best of our knowledge, complexes **3** are the first monomeric group 6 mononitrosyl Schrock-type alkylidene complexes to have been isolated. A few Fischer-type complexes are known, e.g.: (a) CpCr(NO)(CO)(=CPh<sub>2</sub>) (Herrmann, W. A.; Hubbard, J. L.; Bernal, I.; Korp, J. D.; Haymore, B. L.; Hillhouse, G. L. *Inorg. Chem.* 1984, 23, 2978). (b) CpM(NO)(CO)(=C(O)Me)(Ph) (M = Cr, Mo, W). Fischer, E. O. *Pure Appl. Chem.* 1970, 24, 407.

The rate-determining formation of CpMo(NO)(=CHCMe<sub>3</sub>) from **1** is supported by kinetic data. Thermolysis of CpMo(NO)(CD<sub>2</sub>CMe<sub>3</sub>)<sub>2</sub>, **1-d<sub>4</sub>**,<sup>12</sup> in the presence of trapping ligands, L, is clearly first-order in **1** and zero-order in L. The decomposition of **1-d<sub>4</sub>** in CH<sub>2</sub>Cl<sub>2</sub> at 40 °C in the presence of 3.56, 5.24, 10.17, or 13.64 equiv of PPh<sub>2</sub>Me, 6.49 equiv of PPh<sub>3</sub>, or 9.00 equiv of P(*p*-tolyl)<sub>3</sub> affords *k*<sub>obsd</sub> values of 2.81 ± 0.3 × 10<sup>-4</sup> s<sup>-1</sup>. Additionally, an Eyring plot (15–45 °C) for the **1-d<sub>4</sub>** to **3a-d<sub>1</sub>** transformation yields values of Δ*H*<sup>‡</sup> = +79.2 kJ mol<sup>-1</sup> and Δ*S*<sup>‡</sup> = –14.4 eu. These parameters imply the existence of a highly ordered transition state.<sup>13</sup>

Since the formation of CpMo(NO)(=CHCMe<sub>3</sub>) is rate-determining, simple coupling of two molecules of CpMo(NO)(=CHCMe<sub>3</sub>) is not a mechanistic path to **2**. Instead, the transient alkylidene monomer in all likelihood forms an adduct with a second molecule of **1**, which then eliminates neopentane and rearranges to produce **2**. Just why the dimer adopts such an asymmetric structure remains to be ascertained. The characteristic reactivity of the transient CpMo(NO)(=CHCMe<sub>3</sub>) fragment with unsaturated organic entities capable of coupling with the alkylidene ligand is also currently being investigated.<sup>14</sup>

**Acknowledgment.** We are grateful to NSERC for support of this work and Prof. Malcolm Chisholm for providing us with a procedure for the preparation of Me<sub>3</sub>CCD<sub>2</sub>Br.

**Supplementary Material Available:** Experimental procedures and characterization of complexes **1–3** and full details of the crystal structure analyses including associated tables for **2** and **3a** (46 pages); tables of measured and calculated structure factor amplitudes for **2** and **3a** (52 pages). Ordering information is given on any current masthead page.

(11) Kiel, W. A.; Lin, G.-Y.; Constable, A. G.; McCormick, F. B.; Strouse, C. E.; Eisenstein, O.; Gladysz, J. A. *J. Am. Chem. Soc.* 1982, 104, 4865.

(12) Kinetic analyses were effected with **1-d<sub>4</sub>** since it is more thermally stable than **1** and hence more amenable to study. Its markedly increased thermal stability is also consistent with the view that its primary pathway for thermal decomposition involves α-H(D) elimination as the rate-determining step.

(13) Wood, C. D.; McLain, S. J.; Schrock, R. R. *J. Am. Chem. Soc.* 1979, 101, 3210 and references therein.

(14) For a recent example of this type of chemistry, see: Garrett, K. E.; Sheridan, J. B.; Pourreau, D. B.; Feng, W. C.; Geoffroy, G. L.; Staley, D. L.; Rheingold, A. L. *J. Am. Chem. Soc.* 1989, 111, 8383 and references therein.

## Measurement of Long-Range <sup>13</sup>C–<sup>13</sup>C *J* Couplings in a 20-kDa Protein–Peptide Complex<sup>†</sup>

Ad Bax,\*<sup>‡</sup> David Max,<sup>§</sup> and David Zax<sup>||</sup>

Laboratory of Chemical Physics, National Institute of Diabetes and Digestive and Kidney Diseases  
National Institutes of Health  
Bethesda, Maryland 20892  
Magnex Scientific Ltd., 13–19 Blacklands Way  
Abingdon, OX14 1DY, United Kingdom  
Department of Chemistry, Baker Laboratory  
Cornell University, Ithaca, New York 14853

Received April 1, 1992

<sup>13</sup>C–<sup>13</sup>C three-bond *J* couplings are important carriers of structural information and depend on dihedral angles in a manner similar to *J*<sub>HH</sub> couplings.<sup>1,2</sup> At natural <sup>13</sup>C abundance, the long-range *J*<sub>CC</sub> couplings are difficult to measure because the weak <sup>13</sup>C–<sup>13</sup>C doublets of molecules with coupled <sup>13</sup>C nuclei are dwarfed by the nearly 200 times stronger signal from singlets of

<sup>†</sup> This paper is dedicated to Professor Ray Freeman, Cambridge University, on the occasion of his 60th birthday.

<sup>‡</sup> National Institute of Diabetes and Digestive and Kidney Diseases.

<sup>§</sup> Magnex Scientific Ltd.

<sup>||</sup> Cornell University.

(1) Karplus, M. *J. Phys. Chem.* 1959, 30, 11–15.

(2) Bystrov, V. F. *Prog. NMR Spectrosc.* 1976, 10, 41–81.

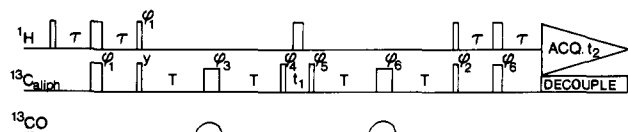


**Figure 1.** Pulse scheme of the  $^1\text{H}$ -detected long-range  $^{13}\text{C}$ - $^{13}\text{C}$  correlation experiment.  $90^\circ$  and  $180^\circ$  pulses are drawn as narrow and wide bars, respectively. The two  $180^\circ$   $^{13}\text{C}_{\text{aliph}}$  pulses applied at the midpoints of the  $2T$  periods are of lower amplitude, with a null in the excitation profile at the carbonyl frequency. Shaped pulses applied to the carbonyl nuclei have a  $180^\circ$  flip angle and do not excite any of the other  $^{13}\text{C}$  nuclei. Note that in principle the pairs of  $180^\circ$   $^{13}\text{C}_{\text{aliph}}$  and  $^{13}\text{CO}$  pulses could be replaced by single nonselective  $180^\circ$  pulses, but in practice the RF field strength obtainable ( $\sim 24$  kHz) is insufficient for this purpose. Delays:  $\tau = 1.5$  ms;  $T = 14.7$  ms. Phase cycling:  $\phi_1 = y, -y; \phi_2 = 2(y), 2(-y); \phi_3 = 2(x), 2(-x), 2(y), 2(-y); \phi_4 = 8(x), 8(-x); \phi_5 = 16(x), 16(-x); \phi_6 = x; \text{acq} = x, 2(-x), x, -x, 2(x), -x$ . Quadrature in the  $t_1$  dimension is obtained using the TPPI-States method with phase incrementation of  $\phi_5, \phi_6,$  and  $\phi_2$ .

molecules with a single  $^{13}\text{C}$ . Although the intense singlet can be suppressed using the INADEQUATE experiment,<sup>3</sup> the use of this method for measurement of long-range couplings remains limited and has never gained widespread popularity.

In  $^{13}\text{C}$ -enriched proteins, direct measurement of such  $J_{\text{CC}}$  values is difficult because of the small magnitude of these couplings relative to the natural line width of the  $^{13}\text{C}$  resonances and because of extensive overlap in the  $^{13}\text{C}$  spectrum. The line width problem is alleviated for methyl groups, which experience reduced dipolar broadening because of rapid rotation about their 3-fold symmetry axis. In addition, the transverse relaxation of methyl carbons in proteins is highly nonexponential, and the slowly decaying component of the  $^{13}\text{CH}_3$  magnetization gives rise to a spectral component with a width of only a few hertz, even in proteins with correlation times as long as 10 ns.<sup>4</sup> Here we describe an "in-phase" COSY experiment that correlates the narrow component of the methyl  $^{13}\text{C}$  resonance with  $^{13}\text{C}$  nuclei that have a long-range coupling to this methyl carbon. The intensity of the observed correlation is related to the size of the  $J_{\text{CC}}$  coupling.

The pulse scheme used in the present work is sketched in Figure 1.  $^1\text{H}$  magnetization is transferred via an INEPT sequence<sup>5</sup> to its directly attached carbon. Dephasing caused by both  $^1J_{\text{CC}}$  and  $^nJ_{\text{CC}}$  couplings takes place during the following period of total duration  $2T$ .  $^1J_{\text{CC}}$  couplings involving methyl groups are quite uniform:  $\sim 37.5$  Hz for Thr and  $\sim 34$  Hz for Ala, Leu, Ile, and Val. Therefore, for Ala, Leu, Ile, and Val the effect of  $^1J_{\text{CC}}$  coupling is refocused at the end of the first  $2T$  period by adjusting  $2T$  to  $1/{}^1J_{\text{CC}}$  (29.4 ms). However, in the presence of a long-range coupling  $^nJ_{\text{CC}}$  to carbon  $n$ , dephasing proportional to  $\sin(2\pi{}^nJ_{\text{CC}}T)$  is caused by the  $^nJ_{\text{CC}}$  coupling. The antiphase  $^{13}\text{C}$  methyl group magnetization at this time is converted into antiphase transverse magnetization of its coupling partner,  $n$ . After a short  $t_1$  evolution period (0–8 ms), this magnetization is transferred back to the methyl carbon, and after another  $2T$  refocusing period, this magnetization is transferred to the methyl protons for detection. In the 2D spectrum, the methyl protons show a correlation to the long-range-coupled carbon with integrated intensity proportional to  $\sin^2(2\pi{}^nJ_{\text{CC}}T) \prod_{m \neq n} \cos^2(2\pi{}^mJ_{\text{CC}}T)$  and a correlation with intensity proportional to  $\prod_m \cos^2(2\pi{}^mJ_{\text{CC}}T)$  for the methyl carbon itself, where  $^mJ_{\text{CC}}$  denotes the coupling between the methyl carbon considered and other carbons,  $m$ . Therefore, the ratio of the integrated peak volumes equals  $\tan^2(2\pi{}^nJ_{\text{CC}}T)$ .

Because for threonine  $^1J(\text{C}_\beta\text{C}_\gamma)$  ( $\sim 37.5$  Hz) is considerably larger than the "tuned" value of 34 Hz, spurious correlations via  $^1J(\text{C}_\beta\text{C}_\gamma)$  are expected (Figure 2C), with intensities corresponding to those of long-range correlations via  $37.5 - 34 = 3.5$  Hz couplings.

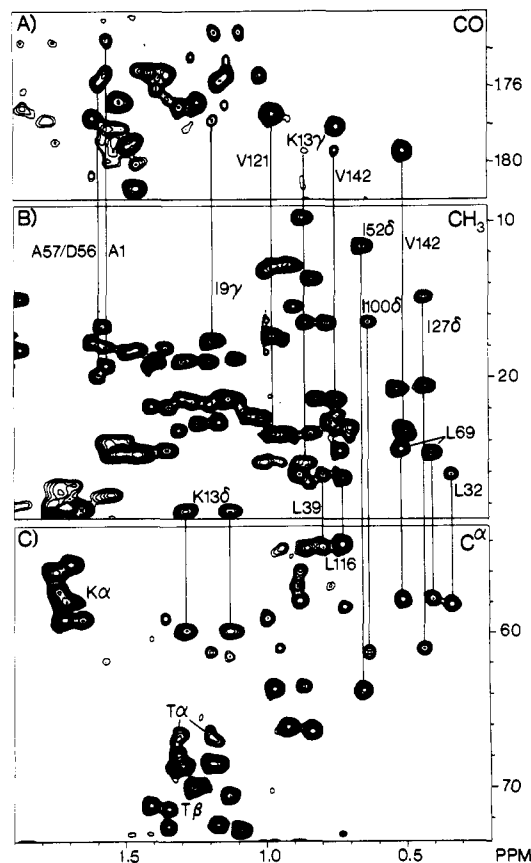


**Figure 2.**  $^1\text{H}$ -detected 2D  $^{13}\text{C}$ - $^{13}\text{C}$  long-range correlation spectrum of  $^{13}\text{C}$ -enriched calmodulin, complexed with a 26-residue peptide. The methyl region (panel B) corresponds to magnetization not transferred via long-range couplings and would be equivalent to the diagonal in a  $^{13}\text{C}$ -detected version of the experiment. Correlations to the carbonyls are shown in panel A and correlations to the  $\text{C}_\alpha$  region in panel C. The methyl region is plotted at a contour level 10 times higher than the cross-peak regions. The intensity of the overlapping signals in the methyl region is obtained from a reference "constant-time"  $^1\text{H}$ - $^{13}\text{C}$  correlation, recorded with a "constant-time" evolution period set to  $4T$  and yielding very high  $^{13}\text{C}$  resolution. For all resonances resolved in panel B, a very good direct proportionality between the integrated intensity in the low-resolution display of Figure 2B and the high-resolution reference spectrum was established, thus yielding accurate intensities for methyl resonances that are overlapping in panel B but resolved in the reference spectrum. The spectrum was recorded on a Bruker AMX-600 spectrometer, and the total accumulation time was 7.5 h for the spectrum shown and 2 h for the reference spectrum.

**Table I.**  $^2J_{\text{CC}}$  and  $^3J_{\text{CC}}$   $^{13}\text{C}$ - $^{13}\text{C}$  Couplings<sup>b</sup> for Methyl Groups of the Calmodulin Isoleucine Residues in the CaM-M13 Complex

residue	$^2J_{\text{C}_\beta\text{C}_\alpha}$	$^3J_{\text{C}_\beta\text{CO}}$	$^3J_{\text{C}_\beta\text{C}_\alpha}$
Ile-9	<1.0	1.2	3.0
Ile-27	1.7	<1.3	<1.7
Ile-52	<1.1	<1.1	<2.1
Ile-63	<1.3	<i>a</i>	2.7
Ile-85	<i>a</i>	<0.9	3.1
Ile-100	1.9	<1.5	3.0
Ile-125	<0.8	<0.8	1.9
Ile-130	<i>a</i>	<i>a</i>	2.9

<sup>a</sup> Not determined because of overlap. <sup>b</sup>  $J$  couplings are in hertz, with an estimated error of 0.2 Hz.

Figure 2 shows the regions of interest of the spectrum obtained with the 2D version of the scheme of Figure 1 for a 1 mM solution of the protein calmodulin complexed with an equimolar amount of a tightly binding 26-residue peptide fragment. Values for  $^nJ_{\text{CC}}$  of the isoleucine residues derived from this spectrum are reported in Table I. The remainder is available as supplementary material. Large values for  $^3J_{\text{CC}}$  ( $\sim 3$  Hz) correspond to trans conformations, whereas small values ( $<1.2$  Hz) correspond to gauche. Inter-

(3) Bax, A.; Kempsell, S. P.; Freeman, R. *J. Am. Chem. Soc.* **1980**, *102*, 4849–4851.

(4) Nicholson, L. K.; Kay, L. E.; Baldissari, D. M.; Arango, J.; Young, P. E.; Bax, A.; Torchia, D. A. *Biochemistry* **1992**, *31*, 5253–5263.

(5) Morris, G. A.; Freeman, R. *J. Am. Chem. Soc.* **1979**, *101*, 760–761.

mediate values are expected if rotamer averaging takes place or if the rotamer is skewed relative to its natural preference. Clearly, such couplings provide useful structural information. For example, for Ile-9, the  $\chi_1$  torsion angle is either  $60^\circ$  or  $-60^\circ$  ( $60^\circ$  based on HNHB<sup>6</sup> and HN(CO)HB<sup>7</sup> experiments), and  $\chi_2$  is  $180^\circ$ . As can be seen from Table I, and as expected on the basis of a statistical search of the protein data bank,<sup>8</sup>  $\chi_2$  is  $180^\circ$  for most Ile residues in the protein-peptide complex. A large number of similar dihedral constraints can be derived from the  $^3J_{CC}$  couplings measured for other residues. Two-bond  $J_{CC}$  couplings may yield additional information, analogous to  $^2J_{CH}$  couplings,<sup>9</sup> but they tend to be quite small; the largest measured value in calmodulin was 1.9 Hz.

The method presented here demonstrates a convenient way for obtaining information on the conformation of methyl group containing side chains in proteins. The spectrum can be recorded in a 2D fashion but also is easily extended into a 3D experiment with a "constant-time"  $^{13}C$  evolution period<sup>10</sup> by replacing the first and second  $T$  periods by  $T + t_2$  and  $T - t_2$ , respectively. The information provided in the present experiment complements that of other approaches which measure long-range  $^1H$ - $^{13}C$  couplings.<sup>9,11</sup>

**Acknowledgment.**  $^{13}C$  assignments used in this study were kindly provided by Dr. M. Ikura. Spectra to confirm these assignments were recorded by Dr. S. Grzesiek. This work was supported by the intramural AIDS targeted Anti-Viral Program of the Office of the Director of the National Institutes of Health.

**Supplementary Material Available:** A table with 104 multiple bond  $^{13}C$ - $^{13}C$  couplings, derived from the spectrum shown in Figure 2 (2 pages). Ordering information is given on any current masthead page.

(6) Archer, S. J.; Ikura, M.; Torchia, D. A.; Bax, A. *J. Magn. Reson.* **1991**, *95*, 636-641.

(7) Grzesiek, S.; Ikura, M.; Clore, G. M.; Gronenborn, A. M.; Bax, A. *J. Magn. Reson.* **1992**, *96*, 215-221.

(8) James, M. N. G.; Sielecki, A. R. *J. Mol. Biol.* **1983**, *163*, 299-361.

(9) Hansen, P. E. *Biochemistry* **1991**, *30*, 10457-10466.

(10) Vuister, G. W.; Bax, A. *J. Magn. Reson.* **1992**, *98*, 428-435.

(11) Sattler, M.; Schwalbe, H.; Griesinger, C. *J. Am. Chem. Soc.* **1992**, *114*, 1126-1127.

## Is 2,3,5,6-Tetrakis(methylene)bicyclo[2.2.0]hexane the Product of Photolyzing 7-Oxa[2.2.1]hericene?

Ruifeng Liu,\* Xuefeng Zhou, and James F. Hinton

Department of Chemistry and Biochemistry  
University of Arkansas, Fayetteville, Arkansas 72701

Received April 10, 1992

Whether the ground state of 1,2,4,5-tetrakis(methylene)benzene (TMB) biradical (1) is a singlet or a triplet is of considerable interest.<sup>1-5</sup> This molecule belongs to the class of "disjoint"<sup>6-11</sup>

(1) Lahti, P. M.; Rossi, A.; Berson, J. A. *J. Am. Chem. Soc.* **1985**, *107*, 2273.

(2) Lahti, P. M.; Rossi, A.; Berson, J. A. *J. Am. Chem. Soc.* **1985**, *107*, 4362.

(3) Du, P.; Hrovat, D. A.; Borden, W. T.; Lahti, P. M.; Rossi, A.; Berson, J. A. *J. Am. Chem. Soc.* **1986**, *108*, 5072.

(4) Roth, W. R.; Langer, R.; Bartmann, M.; Stevermann, B.; Maier, G.; Reisenauer, H. P.; Sustmann, R.; Müller, W. *Angew. Chem., Int. Ed. Engl.* **1987**, *26*, 256.

(5) Reynolds, J. H.; Berson, J. A.; Kumashiro, K. K.; Duchamp, J. C.; Zilm, K. W.; Rubello, A.; Vogel, P. *J. Am. Chem. Soc.* **1992**, *114*, 763.

(6) Borden, W. T.; Davidson, E. R. *J. Am. Chem. Soc.* **1977**, *99*, 4587.

(7) Kollmar, H.; Staemmler, V. *Theor. Chim. Acta* **1978**, *48*, 223.

(8) Borden, W. T.; Davidson, E. R.; Hart, P. J. *J. Am. Chem. Soc.* **1978**, *100*, 388.

(9) Buenker, R. J.; Peyerimhoff, S. D. *J. Chem. Phys.* **1968**, *48*, 354.

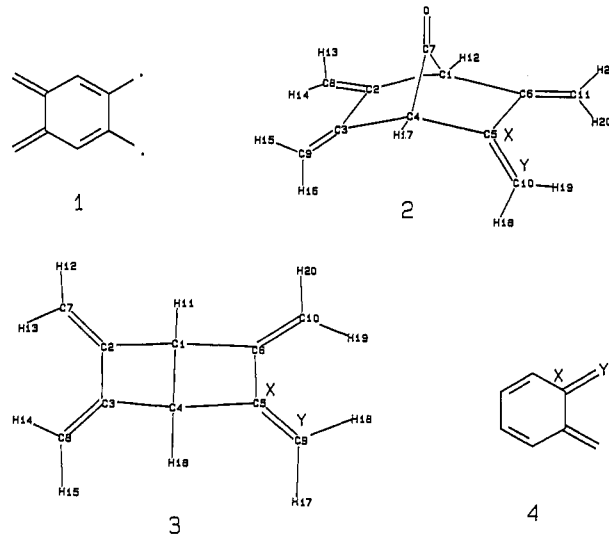
(10) Dixon, D. A.; Foster, R.; Halgren, T.; Lipscomb, W. N. *J. Am. Chem. Soc.* **1978**, *100*, 1359.

Table I. Optimized Geometrical Parameters

TMBCH <sup>a</sup> (3)			7-oxa[2.2.1]hericene (2)		
parameter <sup>b</sup>	4-21G	6-31G**	parameter <sup>b</sup>	4-21G	6-31G**
$R_{12}$	1.539	1.526	$R_{12}$	1.533	1.527
$R_{23}$	1.499	1.490	$R_{23}$	1.502	1.499
$R_{14}$	1.598	1.573	$d_{14}$	2.309	2.300
$R_{27}$	1.312	1.317	$R_{28}$	1.314	1.319
$R_{1,11}$	1.076	1.082	$R_{1,12}$	1.074	1.079
$R_{7,12}$	1.073	1.076	$R_{8,13}$	1.072	1.075
$R_{7,13}$	1.073	1.076	$R_{8,14}$	1.072	1.075
$\angle 11,1,4$	124.3	123.6	$\angle 12,1,7$	117.5	117.2
$\angle 11,1,2$	118.7	117.7	$\angle 12,1,2$	116.1	116.1
$\angle 2,1,6$	111.8	114.5	$\angle 2,1,6$	106.1	107.2
$\angle 7,2,1$	133.8	133.7	$\angle 8,2,1$	126.4	126.2
$\angle 7,2,3$	134.3	134.7	$\angle 8,2,3$	128.3	128.6
$\angle 1,2,3$	91.8	91.6	$\angle 1,2,3$	105.3	105.2
$\angle 2,1,4$	88.2	88.4	$\angle 2,1,7$	99.2	98.9
$\angle 2,1,4,5$	111.9	114.6	$\angle 2,1,4,5$	111.8	113.0
$\angle 7,2,3,4$	177.8	117.4	$\angle 8,2,3,4$	-179.0	-178.5
			$\angle 1,7,4$	97.2	97.4
			$\angle 7,1,2,3$	33.7	33.8
			$R_{CO}$	1.200	1.181

<sup>a</sup> TMBCH: 2,3,5,6-tetrakis(methylene)bicyclo[2.2.0]hexane. <sup>b</sup> The numbering of atoms is given in structures 2 and 3.

biradicals which are expected on the basis of Hückel MO theory to have close-lying singlet and triplet states. Both semiempirical<sup>1</sup> and ab initio calculations<sup>2,3</sup> predict a singlet ground state for 1 with the triplet 5-7 kcal/mol higher at the highest level of theory applied.<sup>3</sup> However, a recent UV-vis and ESR study on the photoproduct of 7-oxa[2.2.1]hericene (2) favored a triplet ground state for TMB.<sup>4</sup>



More recently, Berson et al.<sup>5</sup> reported experimental studies on the same photoreaction and concluded that the carrier of the ESR and UV-vis signals, reported in ref 4, is not the same species. By photolyzing 2,3-( $^{13}CH_2$ )<sub>2</sub>-labeled 2, they observed a new  $^{13}C$  NMR signal at 113 ppm which is 8 ppm from that of the precursor, and its intensity increase was matched quantitatively by the intensity decrease of the precursor signal. On the basis of comparison of the chemical shift of the new signal with those of the singlet biradicals, e.g., 3,4-bis(methylene)furan (102 ppm)<sup>12</sup> and 3,4-bis(methylene)thiophene (105 ppm),<sup>13,14</sup> and the agreement between the calculated values<sup>3</sup> of  $\lambda_{max}$  and  $\epsilon$  for the  $^1A_g \rightarrow ^1B_{3u}$  transition of the singlet TMB and the observed results,<sup>5</sup> they concluded that a kinetically stable singlet TMB is responsible for

(11) Seeger, D. E.; Berson, J. A. *J. Am. Chem. Soc.* **1983**, *105*, 5146.

(12) Zilm, K. W.; Merrill, R. A.; Greenberg, M. M.; Berson, J. A. *J. Am. Chem. Soc.* **1987**, *109*, 1567.

(13) Zilm, K. W.; Merrill, R. A.; Webb, G. G.; Greenberg, M. M.; Berson, J. A. *J. Am. Chem. Soc.* **1989**, *111*, 1533.

(14) Greenberg, M. M.; Blackstock, S. C.; Berson, J. A.; Merrill, R. A.; Duchamp, J. C.; Zilm, K. W. *J. Am. Chem. Soc.* **1991**, *113*, 2318.